Electrochemical Preparation and Properties of Polypyrrole and Its Blend with Poly(vinyl sulfonate) Doped with Perchlorate Anions

Abbas Emamgholizadeh, Maryam Khoshroo, Abdollah Omrani, Abbas A. Rostami

Department of Chemistry, University of Mazandaran, P. O. Box 453, Babolsar, Iran

Received 12 April 2009; accepted 14 July 2009
DOI 10.1002/app.32092
Published online 3 May 2010 in Wiley InterScience (www.interscience.wiley.com).

ABSTRACT: In this article, we report polypyrrole (PPy)/poly(vinyl sulfonate) (PVS) and PPy/perchlorate (ClO_4^-) composite films generated by the electrochemical oxidation of pyrrole on a glassy carbon electrode (GCE) in an aqueous solution. The response of the produced films to an applied potential at 0.7 V was obtained by a cyclic voltammetry study in acetonitrile media. The films were significantly similar in their electrochemical behavior when ClO_4^- ions doped during the redox process. We concluded that with an increasing number of cycles, the anodic current increased because the number of the electroactive participants transported in the copolymer matrix was increased. Theoretical studies based on the Nernst and Butler–Volmer equations indicated that the ClO_4^- ion was transported during the oxidation/reduction process of the PPY/PVS and PPY/ClO_4^- films. The produced films were characterized further by means of IR spectroscopy, electrochemical impedance spectroscopy, and scanning electron microscopy to verify that the anion of ClO_4^- was doped into the copolymer matrix as well. © 2010 Wiley Periodicals, Inc. J Appl Polym Sci 117: 3107–3113, 2010

Key words: blends; conducting polymers; electrochemistry; electron microscopy; polypyrroles

INTRODUCTION

In recent years, there has been increasing interest in the electrical conduction of polymers. Various aromatic compounds can be polymerized by electrochemical oxidation in solutions containing a supporting electrolyte.[1] The actuating capabilities of conducting polymers, such as polypyrrole (PPy), are being actively investigated.[2] Polymer movement results by volume changes that occur upon doping and dedoping under electrochemical control. With small mobile anions (A^-), a reversible volume increase can occur during PPy oxidation as anions and associated solvent molecules move into the polymer backbone:

$$PPy + A^- \rightleftarrows PPy^+(A^-) + e^- \quad (1)$$

With alternative solvents or when large immobile anions, such as dodecyl benzene sulfonate, are incorporated during oxidative polymerization, swelling occurs during polymer reduction through the movement of mobile cations (C^+) and associated solvent as follows:[3,4]

$$PPy^+(A^-) + C^+ + e^- \rightleftarrows PPy(A^-)(C^+) \quad (2)$$

Correspondence to: A. Omrani (omrani@umz.ac.ir).

Journal of Applied Polymer Science, Vol. 117, 3107–3113 (2010)

As the charging/discharging process is actually the doping/dedoping procedure of counterions (anions), the anions in the preparing and testing solution have a decisive impact on the electrochemical properties of PPy films. Wang et al.[5] reported that PPy doped with perchlorate (ClO_4^-) had a higher specific capacitance than that of PPy doped with NO_3^-. Moreover, the doping process could be attained by chemical and electrochemical methods to result in nonstoichiometric compounds. However, the electrochemical way allows full control of the attained doping level. The weight percentage of anions and solvent in the polymer could be electrochemically changed, depending on both the electric potential imposed onto the polymer and the polarization time. PPy synthesis by the electrochemical oxidation of pyrrole monomers is a well-known and well-controlled method. Anions of different sizes can be used to dope PPy during the polymerization process. Examples of these anions include (1) small anions, such as ClO_4^-, NO_3^-, and Cl^-; (2) huge anions, such as poly(styrene sulfonate) (PSS) or poly(vinyl sulfonate) (PVS); and (3) medium-sized anions, such as *p*-toluensulfonate or benzenesulfonate.[6,7] Smyrl and coworkers[8,9] reported that PPy films doped exclusively with small anions showed anion movement during the redox process, whereas in PPy films doped with PVS or PSS, cations were inserted and expelled from the polymeric matrix. Otero et al.[10] revealed that different applied

potentials and solvent and anionic radii could induce various electrochemical relaxations. Solvent molecules can be transported inside the polymer during the redox process, and so, depending on the solvent–ion and solvent–polymer interactions, ionic transport may be very different. Finally, anion or cation movement is strongly dependent on the structural disparities existing in PPy films.[11] The solvent used for film growth and electrochemical studies can affect the film morphology and counterion transport behavior.[12,13] In one case, the vapor-sensing capabilities of a polymer film were more selective for methanol vapors when the polymer was grown from a methanol solution instead of acetonitrile (AN).[14] Various experimental techniques, such as cyclic voltammetry (CV), electrochemical quartz crystal microbalance measurements, energy-dispersive X-rays (EDX), probe beam deflection, and electron paramagnetic resonance, have been used to determine the nature of ionic transport during its oxidation or reduction process.[6,11] In this research, we confirmed that ClO_4^- anions become the main mobile species during the redox process of PPy/PVS blends.

EXPERIMENTAL

Materials

The pyrrole monomer (Fluka; >99%, Buchs, Switzerland), (Aldrich, Munich, Germany), and (Merck, Darmstadt, Germany) was distilled two times before electropolymerization. All other reagents, including sodium PVS (Aldrich), $LiClO_4^-$ (Merck), and AN (Merck), were used without any treatment or further purification. Bidistilled water was used for the preparation of solutions.

Electrode preparation and electropolymerization

The used working electrode was a glassy carbon (GC) electrode. A platinum wire was also used as a counter electrode (CE). All potentials are reported versus the reference electrode Ag/AgCl (saturated KCl). We cleaned the GC electrode surface by successively polishing it with a 0.05-μm alumina slurry. After each polishing, the electrode was carefully washed with distilled water. PPy/PVS and PPy/ClO_4^- films were generated by electrochemical oxidation on the GC electrodes at 0.7 V versus (Ag/AgCl) in aqueous solutions of 0.1*M* pyrrole with 0.05*M* PVS–Na and 0.1*M* $LiClO_4$. A schematic set up of the used treatment is shown in Figure 1. The polymerization charges were 70 mC/cm^2 for the PPy/PVS and PPy/ClO_4^- films. After generation, the films were washed with water and AN. All solutions were purged with argon gas for 15 min before the electrochemical tests.

Instrumentation and procedure used

Electrochemical measurements were performed in a one-compartment cell with a three-electrode configuration. CV study was conducted with a potentiostat/galvanostat (EG&G model 263 A, Oak Ridge, TN) with an electrochemical set up that controlled by M 270 software. Electrochemical impedance spectroscopy (EIS) was performed with a frequency response detector (EG&G model 1025) with electrochemical set ups and under the control of M 398 software. An alternating-current voltage of 5 mV in amplitude with a frequency range from 50 mHz to 65 kHz was applied for the EIS measurements. The PPy/PVS films doped with ClO_4^- anion at direct-current (dc) potentials of 1.1, 0.8, 0.7, and 0.6 V in 0.1*M* $LiClO_4$/AN were tested for the doping process assessment in the same frequency range. Scanning electron microscopy (SEM) images of the produced doped films were taken with Vega 5135 (Tescan, Brno, Czech Republic) and HV (high potential) 1500-V instrument at various magnifications. Sample films for imaging were grown on the GC electrode. A Fourier transform infrared (FTIR) spectroscopy study was carried out with a Bruker spectrophotometer (Vector 22, Bremen, Germany) equipped with OPUS software.

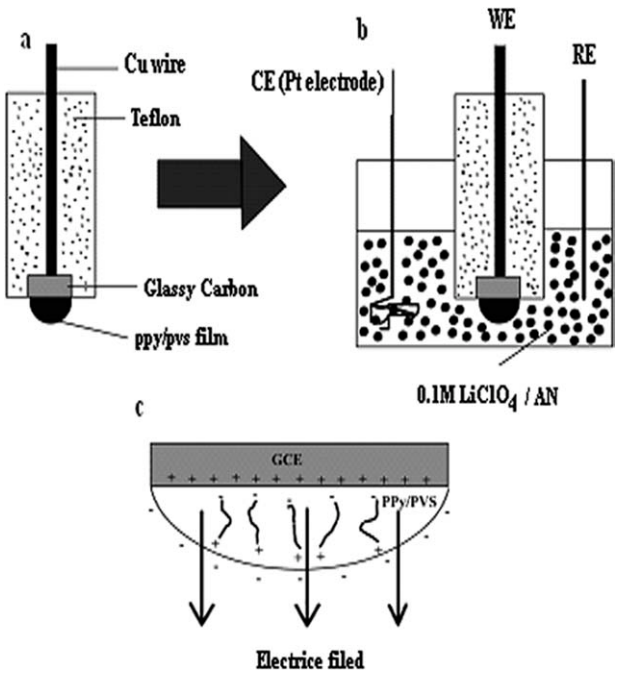

Figure 1 (a) GC, (b) three-electrode cell, and (c) preferential orientation of PPy/PVS under an electric field. WE, working electrode; RE, reference electrode; AE, auxiliary electrode; GCE, glassy carbon electrode; CE, counter electrode.

RESULTS AND DISCUSSION

CV of the PPy/ClO_4^- and PPy/PVS films

The PPy/ClO_4^- film was grown with the potentiostatic technique. Figure 2 shows 10 consecutive voltammograms, from −1.5 to 1.6 V, preformed on a

PPy/ClO_4^- film in a 0.1*M* $LiClO_4$/AN solution at a scan speed of 0.8 V/s. The charge needed for the reduction or oxidization of the PPy/ClO_4^- film was 0.8 C.[15] In the first cathodic voltammogram, we did not see a cathodic peak, but in the next consecutive cycles, a cathodic peak was observed clearly at −0.4 V; this peak gradually shifted toward higher potentials, as shown in Figure 2.

The charge measured by integration of the anodic peak was 9.02 mC/cm^2 for the 10th cycle, and oxidation of the PPY/PVS film occurred at 0.4 V. The voltammetric behavior of the PPy/PVS film in the same electrolyte solution and in the same potential range is depicted in Figure 3.

Although a similar polymerization charge was used to synthesize the both films (PPy/ClO_4^- and PPy/PVS), the voltammetric behavior of the PPy/PVS film was quite different. During the 1st to the 10th cycle, the anodic charge changed from 0.9 to 8.56 mC/cm^2, and then, it reached a voltammetric steady state. The anodic peak potential shift to higher potentials was also observed for the 10 consecutive cycles, which finally remained constant when the steady state was reached. The anodic charge for the PPy/PVS film after the steady state was reached (in the 12th cycle in Fig. 3) was quite similar to the charge measured for the PPy/ClO_4^- film in the 10th cycle. The charge measured in the voltammetric peaks for PPy/PVS tended to resemble the PPy/ClO_4^- charge with an increasing the number of cycles. A similar increase in the anodic peaks was found when PPy/PBS {copoly[pyrrole-*N*-(butylsulfonate)]} films were cycled in a 0.1*M* $LiClO_4$/AN solution.[7] In this case, the increase was attributed to a replacement of the bulky $(Bu)_4N^+$ cation by the small Li^+ cation. The electrochemical behavior of PPy doped with the large and small anions of PSS and ClO_4^- was also investigated in 0.1*M* solution of sodium poly(styrene sulfonate) and $N(Bu)_4Br$, respectively. The PPy/PSS films exhibited predominantly cation exchange, whereas in the PPy/ClO_4^- films reduced in $N(Bu)_4Br$, only anion exchange was possible.[16] Noticeably, in this study, a small cation (Li^+) in the polymerization process of the PPy/PVS polymer was used. The values of the formal potentials at CV voltammogram maximums for the PPy/PVS blend were more negative than that of the PPy/ClO_4^- films. Peak separation for the PPy/PVS-based copolymers increased with the number of voltammetric cycles to become even higher than that obtained for the polymers doped with ClO_4^- when the steady state was reached. This result was attributed to a slowing down of electrolyte motion in the polyanionic blend during the charging/discharging process. To obtain further information about the electrochemical behavior of the PPy/PVS copolymer films in AN medium, a negative potential of −2.1 V was reached. Considerable changes in their voltammograms with higher anodic peaks and greater anodic charges were observed. With a potential of −2.1 V as the cathodic potential limit, only eight cycles were required to reach a steady voltammogram. Figure 4 illustrates the voltammetric behavior of the PPY/PVS film by changing the anodic limit after stable peaks were reached with −0.8 V as the final potential (E_f).

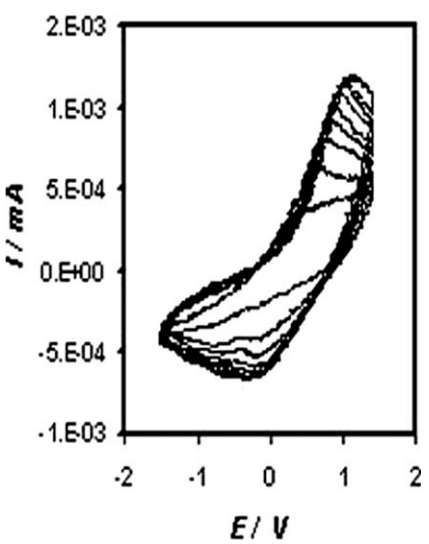

Figure 2 Cyclic voltammograms of the PPy/ClO_4^- polymer in a 0.1*M* $LiClO_4$/AN solution with a scan rate of 0.8 V/s. The 10th consecutives cycles are shown (E_i = +1.6 to E_f = −1.5 V).

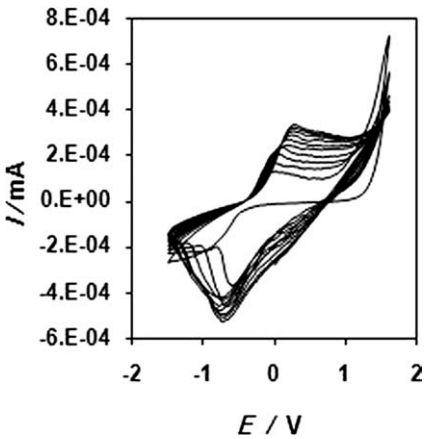

Figure 3 Cyclic voltammograms of the PPy/PVS polymer in a 0.1*M* $LiClO_4$/AN solution with a scan rate of 0.8 V/s. The 25th cycles are shown (E_i = +1.6 V to E_f = −1.5 V).

The current in the anodic peak increased with increasing cathodic limits, accompanied by a small change in the peak potential (E_{peak}) when the limits were −0.8, −1.1, and −1.5 V, but when a strongly negative potential, that is, −2.1 V, was reached, the anodic peak became sharper and shifted to a higher potential (from E_{peak} = +0.75 V to E_{peak} = 0. + 1.02

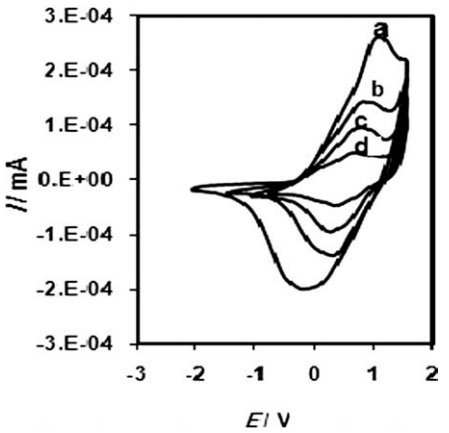

Figure 4 Voltammetric behavior of a PPy/PVS film in a 0.1*M* $LiClO_4$/AN solution with various E_f values: (a) −2.1, (b) −1.5, (c) −1.1, and (d) −0.8 V. The initial potential (E_i) was always adjusted to +1.5 V. The scan rate was 0.8 V/s.

V). Moreover, the anodic charge was also increased up to 8.16 mC/cm^2. Similar anodic shifts and rising charges were observed in the anodic peak when the PPy/ClO_4^- films were cycled up to an E_f of −2.1 V. These results again indicate a similar behavior for the PPy/PVS and PPy/ClO_4^- films under these conditions. The voltammetric behavior described previously resembled an increase in a redox wave for the charging/discharging process of a PPy/PF_6 film in a 0.1*M* $TBAPF_6$/AN because the oxidation voltammetric peak shifted to more positive values by cycling from 1.6 to −2.0 V. This result was associated with a transition from the so-called PPy(II) structure to the PPy(I) structure, which has longer polymer chains.[17] The micromorphological changes in PPy(II) during the voltammetry traces were related to the nature of ion transport, with the cation and anion transport for PPy(II) being gradually replaced by the pure anion transport when PPy(I) was formed. The shift of the anodic peak shown in Figure 4 may then be explained as being due to a restructuring of the PPy/PVS copolymer during cycling, when the polymer formed a more compact structure and made a higher overall potential necessary to flatten the more tilted chains. The redox process involves the exchange of ions and solvent molecules. It is clear that the doping/dedoping process involves changes in the mechanical properties and the electronic structure of the polymer. The structural change in the PPy film took place when the electrolyte ions were transported into or out of the PPy matrix, which was shown by the appearance of current shoulders in the chronoamperograms of potential step experiments.[10] This restructuring may have modified the kind of ionic transfer in the redox process, and the ClO_4^- anions were the main mobile ionic species. Cations, in general, could not be found in the PPy films doped with small inorganic anions, such as Cl^- or ClO_4^-, because of the positive nature of the oxidized main chain, and so the small cation (e.g., Na^+ or Li^+) moved into and out of the polymer matrix to balance the charge of polymer.[18]

Evidence for anionic transport in the AN medium

There was substantial experimental evidence pointing to a prevailing ClO_4^- interchange during the PPy/PVS redox process in the AN solution.

Nernst and Butler–Volmer treatments

As an initial hypothesis, we accepted that, in these types of polymer/polyelectrolyte materials, it was not clear which prevailing species, cation or anion, was transferred during the reverse redox processes. Three different possibilities were considered: (1) there was a prevailing interchange of cations, (2) there was an existing interchange of anions, and (3) both cations and anions participated simultaneously in the oxidation/reduction process. Because the polyelectrolyte remained fixed inside the polymeric material, two basic redox reactions for the prevailing interchange of cations or anions were proposed, as follows:

$$PPy^+PVS^- + Li^+ + e^- \rightleftarrows PPy^0PVS^-Li^+ \quad (3)$$

$$PPy^+PVS^- \times Li^+ \times ClO_4^- + e^- \rightleftarrows PPy^0PVS^- \times Li^+ + ClO_4^- \quad (4)$$

A combination of the aforementioned mechanisms for the charge balance describes the third possibility. In the simplest approximation and with equilibrium conditions, the electrochemical potential (E) for these reactions could be explained by the Nernst equation:

$$E = E^0 + \frac{RT}{nF}\ln\frac{[PPy^+PVS^-][Li^+]}{[PPy^0PVS^- \times Li^+]} = E^0 + \frac{RT}{nF}\ln\frac{[PPy^+PVS^-]}{[PPy^0PVS^- \times Li^+]} + \frac{RT}{nF}\ln[Li^+] \quad (5)$$

$$E = E^0 + \frac{RT}{nF}\ln\frac{[PPy^+PVS^- \times Li^+ \times ClO_4^-]}{[PPy^0PVS^- \times Li^+][ClO_4^-]} = E^0 + \frac{RT}{nF}\ln\frac{[PPy^+PVS^- \times Li^+ \times ClO_4^-]}{[PPy^0PVS^- \times Li^+]} - \frac{RT}{nF}\ln[ClO_4^-] \quad (6)$$

where E^0 is the standard potential. These equations describe the evolution of the redox potentials as a function of the electrolyte concentrations. If cationic interchange prevails, the redox potential versus electrolyte concentration plots will exhibit a semilogarithmic

increase in the potential with the electrolyte concentration. On the other hand, a negative slope is predicted when the interchange of ClO_4^- anions prevails.[19–21] To describe the process kinetically, the Butler–Volmer formalism is more appropriate for the anodic branch of the voltammograms. With regard to the oxidation part of the general process, $R \rightleftarrows O + ne^-$, the Butler–Volmer equation can be expressed as follows:[22]

$$i_a = nFAk^0 C_R \exp[(1-\alpha)n_s f(E - E^0)] \quad (7)$$

$$E = E^0 + \frac{1}{(1-\alpha)n_s f}\ln\frac{i_a}{nFAk^0} - \frac{1}{(1-\alpha)n_s f}\ln C_R \quad (8)$$

where α, k, n_s, i_a and C_R are the transfer coefficient, the standard rate constant, the n value of the rate determining step, the anodic current and the reactive compound's concentration, respectively. For the reaction in eq. (4), this equation can be expressed in the following form:

$$E = E^0 + \frac{1}{(1-\alpha)n_s f}\ln\frac{i_a}{nFAk^0} - \frac{1}{(1-\alpha)n_s f}\ln[PPy^0PVS^- \times Li^+] - \frac{1}{(1-\alpha)n_s f}\ln[ClO_4^-] \quad (9)$$

So, it is clear from the Nernst equation and Butler–Volmer formalism that for the reaction in eq. (4), E is proportional to $-\ln [ClO_4^-]$. Moreover, for the reaction in eq. (3), both equations demonstrate a direct relationship between E and $+\ln [Li^+]$. Consequently, these equations offer a valuable tool for exploring which of the ionic species, cation or anion, prevailed during the charge balancing of the electrochemical processes. To know which ionic species intervened in the redox process of the PPy/PVS films in the AN solution, we conducted a voltammetric study by changing the electrolyte concentration. In this case, the anodic peak potentials in the cyclic voltammograms were considered to be the E potentials. Although this approximation was not completely correct, the polarity of the slopes was the same when the peak potentials in eqs. (5)–(9) were used. Figure 5 shows that the anodic peak shifted toward lower potentials as the electrolyte concentration increased. This resulted in a negative slope when the peak potentials were plotted against ln [$LiClO_4$]. Thus, these results confirmed that the PPy/PVS oxidation was mainly governed by the insertion of ClO_4^- anions.

Effect of the scan rate

The effect of the scan rate on the PPy/PVS films oxidation current was investigated in a 0.1*M* $LiClO_4$/AN solution, and the results are shown in Figure 6. The oxidation current increased with increasing scan rate.

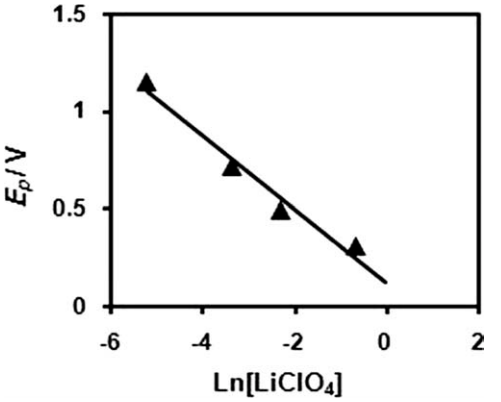

Figure 5 Oxidation peak potentials (E_p) as a function of ln [$LiClO_4$].

An increase in the scan rate was likely to enhance the electron flow. It appeared that the increased collision of electrons resulted in a reduction in the velocity of electrons and led to a saturation in the current.

Effect of increasing the ClO_4^- concentration

Figure 7 shows the effect of the ClO_4^- concentration in the AN medium on the anodic peak current. Concentrations of 0.01, 0.03, 0.1, and 0.3*M* of ClO_4^- anion were used. As shown in Figure 7, with increasing ClO_4^- concentration, there was an increase in the anodic peak current for the resultant polymeric films. The increase in the peak current was due to the fact that an increase in the electroactive surface area of the resulting polymers was deposited at higher current densities.

FTIR of PPy/PVS doped with ClO_4^- and undoped PPy/PVS films

Figure 8(A,B) shows the FTIR spectra of PPy/PVS doped with ClO_4^- and PPy/PVS undoped films

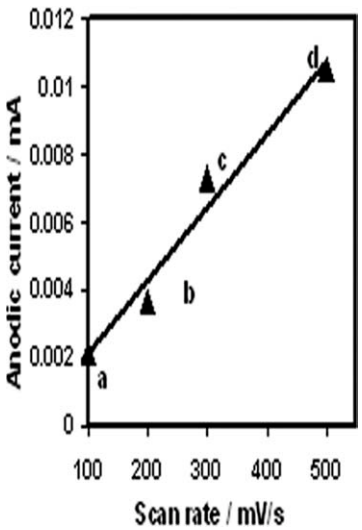

Figure 6 Anodic current of a PPy/PVS film with various scan rates: (a) 100, (b) 200, (c) 300, and (d) 500 mV/s.

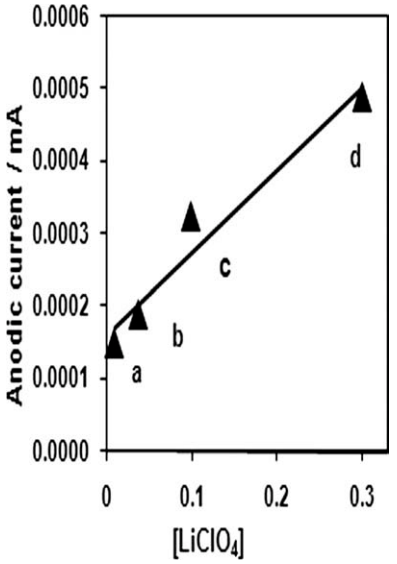

Figure 7 Anodic current of a PPy/PVS film with $LiClO_4$/AN solutions of various concentrations: (a) 0.01, (b) 0.03, (c) 0.1, and (d) 0.3*M*.

coated on GC electrodes. The characteristic peaks for PPy were observed at 1690 cm^{-1} (C=N) and 1360 cm^{-1} (C—N). The 1600 cm^{-1} vibration band was due to the C=C bond associated with C=N stretching and bending vibrations. The vibration at 1170 cm^{-1} was due to the presence of the C=N double bond. Moreover, the vibration peaks at 2343 and 2366 cm^{-1}, which were seen in the FTIR spectra of the

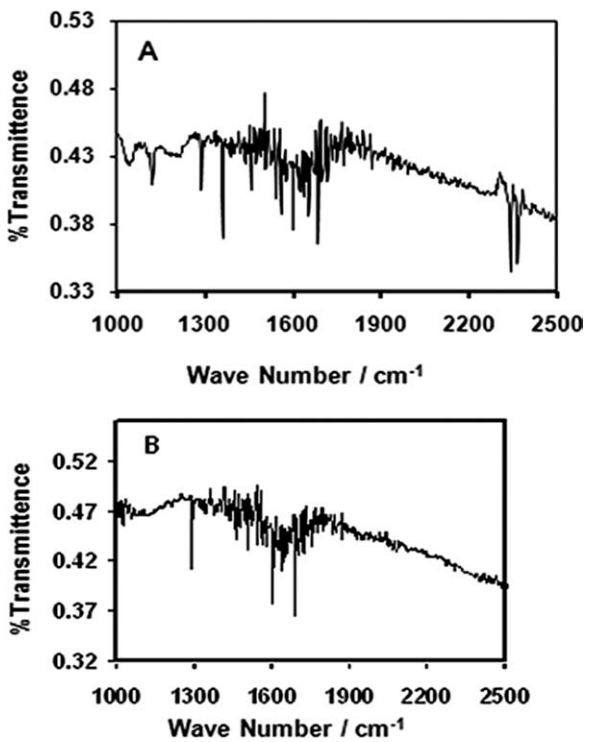

Figure 8 FTIR spectra: transmittance (%) versus wave number (cm^{-1}) for PPy/PVS: (A) doped with ClO_4^- and (B) undoped.

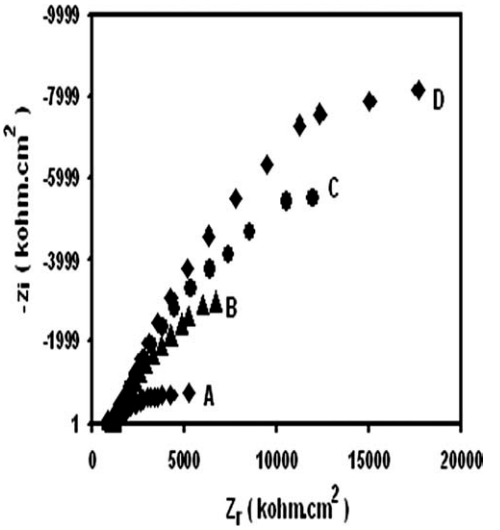

Figure 9 Impedance spectra of PPY/PVS^- doped with ClO_4^- at various dc potentials: (A) 1.1, (B) 0.8, (C) 0.7, and (D) 0.6 V. Z_i, imaginary resistance; Z_r, real resistance.

PPy/PVS blend doped with ClO_4^- film, indicated the dopant peaks of ClO_4^-.

EIS measurements

EIS experiments were conducted to characterize the electrode/polymeric film/electrolyte interface. Figure 9 displays the typical impedance spectra of the PPy/PVS doped with ClO_4^- in 0.1*M* $LiClO_4$/AN recorded at various dc potentials of 1.1, 0.8, 0.7, and 0.6 V at frequency range of 50 mHz to 65 kHz. The semicircle obtained from the high-frequency region was ascribed to the blocking properties of a single electrode, which rendered the faradic process of the ion exchange extremely slow at the polymer/electrolyte interface. The doped PPy/PVS film at the dc potential of 1.1 V had a higher electronic conductivity, that is, a low impedance and vice versa. The charge-transfer resistance (R_{ct}) increased because the higher dopants were exchanged in this case and the film became more stable (see Table I).

Morphology of the produced films

Figure 10 shows the scanning electron micrograph of the doped and undoped PPy/PVS polymeric

TABLE I
Electrical Parameters Calculated from Impedance Spectra in 0.1*M* $LiClO_4$/AN for PPY/PVS Doped with ClO_4^-

E_f (V)	I_a (mA)	E_{dc} (V)	R_{ct} (kΩ cm^2)
−2.1	2.1×10^{-4}	+1.1	7.5×10^2
−1.5	1.4×10^{-4}	+0.8	1.5×10^3
−1.1	9.4×10^{-5}	+0.7	2.0×10^3
−0.8	4.8×10^{-5}	+0.6	2.5×10^3

I_a, anodic current; E_{dc}, applied potential.

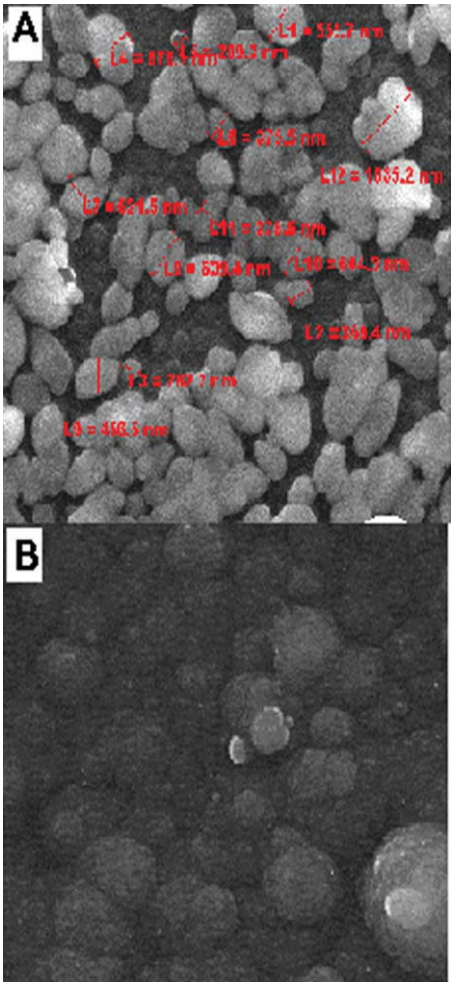

Figure 10 Scanning electron micrographs of (A) PPy/PVS doped with ClO_4^- and (B) undoped PPy/PVS. [Color figure can be viewed in the online issue, which is available at www.interscience.wiley.com.]

films. The doped film showed a tetrahedral morphology. The uniform bright portion in the pictures shows the homogeneity of doping. The particle size in the PPy/PVS doped film was in the range 209.3–1035.2 nm. The undoped PPy/PVS SEM photographs indicate dark nonconducting portions.

CONCLUSIONS

We observed different voltammograms for PPy/PVS and PPy/ClO_4^- polymers in $LiClO_4$/AN. With increasing number of cycles, the voltammograms of PPy/PVS in $LiClO_4$/AN led to similar behavior for both films. The Nernst and Butler–Volmer equations indicated that ClO_4^- was the main mobile species during the redox process for the PPy/PVS films. The gradual increase of redox waves and the positive shift of anodic peaks with cycling supported an irreversible restructuring of the PPy/PVS films. During voltammetric scans, the polymer formed a more compact structure, where the polymeric chains were more crosslinked, and this necessitated a higher overpotential. This overpotential resulted from the additional energy needed to flatten the tilted chains. The doping/dedoping reaction consisted of a reversible exchange of anions, and cation exchange seemed to be absent in this case. With CV, EIS, SEM, and FTIR analyses, it was implied that the small size of the ClO_4^- anion was mobile enough and could be used to improve the conductivity of the PPy films deposited on the GC electrode.

References

1. Ylldlnm, P.; Ktiqtikyavuz, Z. Synth Met 1998, 95, 17.
2. Spinks, G. M.; Liu, L.; Wallace, G. G.; Zhou, D. Adv Funct Mater 2002, 12, 437.
3. Skaarup, S.; Bay, L.; Vidanapathirana, K.; Thybo, S.; Tofte, P.; West, K. Solid State Ionics 2003, 159, 143.
4. Kilmartin, P. A.; Li, K.-C.; Bowmaker, G. A.; Vigar, N. A.; Cooney, R. P.; Jadranka, T.-S. Curr Appl Phys 2006, 6, 567.
5. Wang, J.; Xu, Y.; Chen, X.; Du, X.; Li, X. Acta Phys Chim Sinica 2007, 23, 299.
6. Ohtani, S. T.; Yyoda, A.; Honda, T. K. J Electroanal Chem 1987, 224, 123.
7. Bidan, G.; Ehui, B.; Lapkowski, M. J Phys D 1988, 21, 1043.
8. Lien, M.; Smyrl, W. H.; Morita, M. J Electroanal Chem 1991, 309, 333.
9. Naoi, K.; Lien, M.; Smyrl, W. H. J Electrochem Soc 1991, 138, 440.
10. Otero, T. F.; Grande, H.; Rodriguez, J. Synth Met 1996, 83, 205.
11. Fernandez, R. A. J.; Lopez, C. J. J.; Fernández, O. T. J Phys Chem B 2005, 109, 907.
12. Delabouglise, D. Synth Met 1992, 51, 321.
13. Ren, X.; Pickup, M. J Phys Chem 1993, 97, 5356.
14. Paulse, C. D. J Phys Chem 1988, 92, 7002.
15. Johanson, U.; Marandi, M.; Tamm, T.; Tamm, J. Electrochim Acta 2005, 50, 1523.
16. Plieth, W.; Bund, A.; Rammelt, U.; Neudeck, S.; Duc, L. Electrochim Acta 2006, 51, 2366.
17. Zhou, M.; Pagels, M.; Geschke, B.; Heinze, J. J Phys Chem B 2002, 106, 10065.
18. Kyu, S. M.; Park, J. K.; Yeo, I. H.; Woo, R. H. Synth Met 1999, 99, 219.
19. Ren, X.; Pickup, P. G. J Phys Chem 1993, 97, 5356.
20. Zhong, C.; Oblhofer, K. D. Electrochim Acta 1990, 35, 1971.
21. Levi, M. D.; Lopez, C.; Vieil, E.; Vorotyntsev, M. A. Electrochim Acta 1997, 42, 757.
22. Bard, A. J.; Faulkner, L. R. Electrochemical Methods; Wiley: New York, 2001.